fitted results, as a function of wave vector transfer. By considering interlayer model in Fe-Si system, values of thicknesses and roughnesses for pure Fe, pure Si layer and interlayer were obtained. Interlayer forms due to the strong interdiffusion of Fe and Si into each other. Thickness of interlayer is related to the depth of interdiffusion. Roughness of interlayer is related to the uniformity of interdiffusion. Obtained thickness of interlayer is ~13Å with 4-6Å roughness in each case. This indicates that interlayer formation at Si/Fe interface is independent from the Fe and Si layer thickness. After this interlayer formation no further interdiffusion takes place across Si/Fe interface.

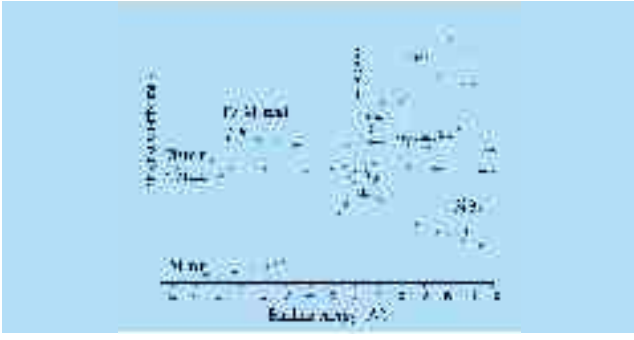

Fig. A.3.1 *Depth profile valence band spectra of bilayer taken at synchrotron Indus-1.*

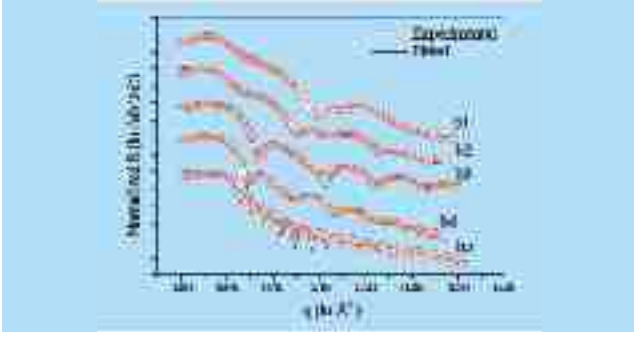

Fig. A.3.2 *GIXRR measurements of bilayers taken at CuKα source.*

Contributed by:
S. R. Naik, S. Rai and G. S. Lodha; lodha@cat.ernet.in

A.4 Design of vacuum ultraviolet polarimeter for Indus-1

Ellipsometric experiments with synchrotron radiation (SR) gives element specific magnetic information about material. To perform these experiments on Indus-1, a VUV polarimeter is designed [*for details please see S. R. Naik, G. S. Lodha, Nuclear Instruments and Methods in Physics Research A, 560 (2006), 211]*. This polarimeter will be installed after the post mirror of toridal grating monochromator based CAT-TGM beamline. To reduce the higher order contamination of SR beam filters will be used. Optical design of polarimeter is completed, which is shown in fig. A.4.1. Polarimeter consists of four-mirror reflector phase retarder and three-mirror reflector linear polarizer.

Polarimetry and ellipsometry require to azimuthally rotate phase retarder and linear polarizer around beam axis. Azimuthal rotation is such that the out going beam position remain unchanged during rotation. In a complete azimuthal rotation phase retarder generates linearly, circularly and elliptically polarized beam, which is shown in fig. A.4.2. In complete azimuthal rotation linear polarizer generates different outgoing intensity pattern, from which the information about the material can be extracted.

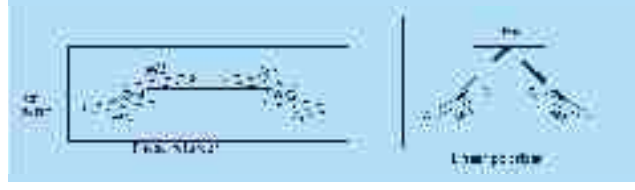

Fig. A.4.1: *Schematic diagram of VUV polarimeter to be installed on CAT-TGM beamline on Indus-1.*

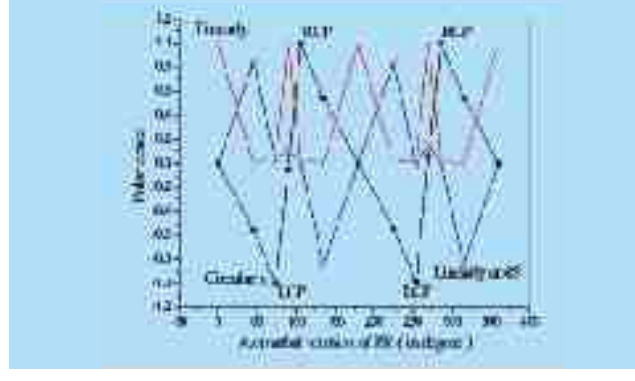

Fig. A.4.2: *Linearly and circularly polarized component of SR beam after PR is drawn as a function of azimuthal rotation of PR.*

Contributed by:
S. R. Naik and G. S. Lodha; lodha@cat.ernet.in

A.5 Analyses of composition at buried interfaces using resonant soft x-ray reflectivity

Normally in x-ray reflectivity (XRR), X-ray photon energy is far away from absorption edges of materials of interest, and the poor contrast in optical constants is not

sufficient to identify the composition of the buried interface at sub-nanometer scale. We have shown possibility of determining phase composition at buried interfaces using soft x-ray resonant reflectivity (SXRRR) tuning photon energy at the absorption edges of constituent element *[for details please see M. Nayak, G. S. Lodha, A.K. Sinha, R.V. Nandedkar, S.A. Shivashankar Applied Physics Letter, 89 (2006)181920]*. We demonstrate this for a Mo-Si multilayer (ML) system, measuring soft x-ray reflectivity by tuning photon energy at Si L-absorption edge (L_{II} =12.34 and L_{III}=12.41nm) using Indus-1 SR. The $[Mo(30Å)/Si(60Å)]_5$ MLs were fabricated on float glass substrate using e-beam evaporation system. Before the SXRRR measurements, the micro-structural parameters were determined with XRR measurements with a Cu target (0.nm). Figure A.5.1 shows the measured and fitted XRR spectra of ML sample. The fitted data for three possible (different) interlayer phase compositions show clearly that conventional XRR is not sensitive to the composition of phases formed at buried interface. This is due to the small difference in optical constants among these compositions.

Figure A.5.2 shows the soft x-ray resonant reflectivity measured spectra using Indus-1 SR. The experimental data are fitted for three different compositions i.e. $MoSi_2$, Mo_5Si_3 and Mo_3Si. For two different photon wavelengths, good agreement between measured and best-fit curve is obtained for the $MoSi_2$ composition, not only near the Bragg peak but also in the Kiessig oscillation region and at grazing angles of incidence around the critical angle of total reflection. The fitted result reveals the formation of $MoSi_2$ composition at the interfaces.

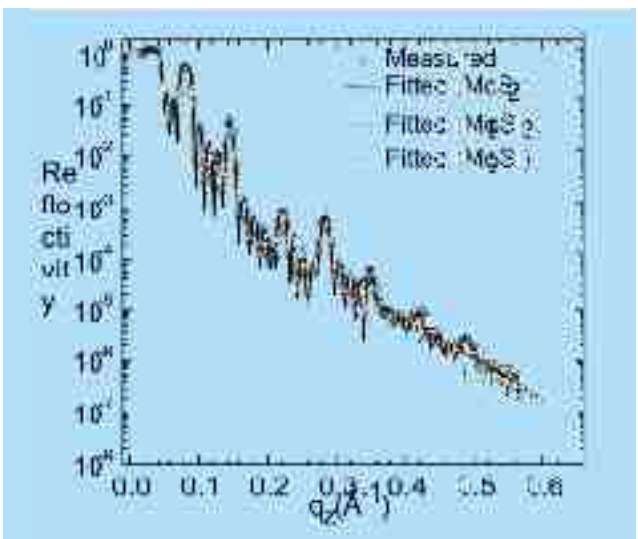

Fig. A.5.1 *XRR spectrum at Cu K wavelength of $[Mo (30Å)/Si(60Å)]_5$ ML.*

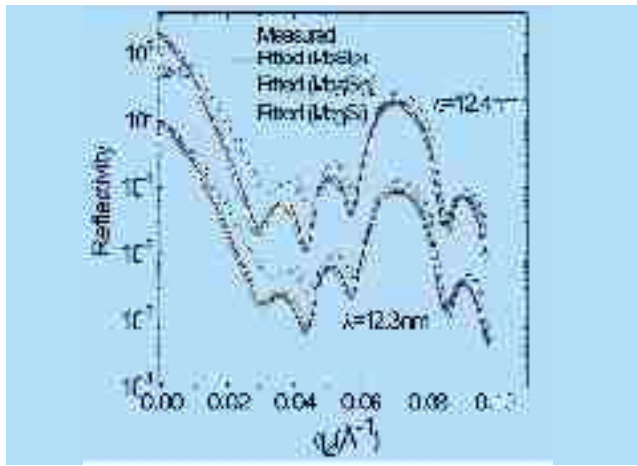

Fig. A.5.2 *Measured and fitted soft x-ray reflectivity of using Indus-1 SR near Si L-edge.*

Contributed by:

M. Nayak; mnayak@cat.ernet.in,G. S. Lodha,
A. K. Sinha and R. V. Nandedkar

A.6 Z-contrast imaging in NbC/Si soft x-ray multilayer

Chemical roughness or the formations of nanocrystallites at the interface of multilayer structure used in soft x-ray mirrors deteriorate the performance of these mirrors. Conventional electron microscopy (CTEM) bright field (BF) imaging is usually not helpful as the strong diffraction contrast arising from the matrix obscures its presence. Since the precipitates differ most often from matrix by elemental content, atomic number (or z) contrast imaging seems to be well suited.

Z-contrast imaging is a common option in a scanning electron microscope (STEM). Here Z-contrast is realized by using an annular dark field (ADF) detector, which collects the electron scattered to high angles. Nano precipitates can be revealed routinely with this technique. Atomic resolution STEM work requires a microscope equipped with a field emission gun, and an exceptionally quite room environment. However, such options are not cheap or commonplace. Although Z-contrast imaging can also be realized in a conventional microscope (CTEM) by hollow cone illumination as well, the illumination cone convergence is limited to about 10 mrad, which is rather small compared to a 50/200mrad collection angle for high angle annular dark field (HAADF) STEM detectors. Hashimoto *(Hashimoto H, Kumao A, Himo K, Endoh H.E., Yotsumoto H& Ono A (1973) Journal of electron Microscopy 22,123)* first demonstrated the possibility to image heavy atoms and clusters by conventional dark field operation.